Bulk electronic structure of Mn_5Ge_3/Ge(111) films by angle-resolved photoemission spectroscopy

W. Ndiaye,[1] M. C. Richter,[1,2] O. Heckmann,[1,2] P. De Padova,[3] J.-M. Mariot,[4] A. Stroppa,[5,6] S. Picozzi,[5,6] W. Wang,[1,7] A. Taleb-Ibrahimi,[8] P. Le Fèvre,[9] F. Bertran,[9] C. Cacho,[10] M. Leandersson,[11] T. Balasubramanian,[11] and K. Hricovini[1,2]

[1]*Laboratoire de Physique des Matériaux et des Surfaces, Université de Cergy-Pontoise, 5 mail Gay-Lussac, 95031 Cergy-Pontoise, France*

[2]*DSM, IRAMIS, Service de Physique et Chimie des Surfaces et des Interfaces, CEA-Saclay, 91191 Gif-sur-Yvette, France*

[3]*CNR, Istituto di Struttura della Materia, via Fosso del Cavaliere, 00133 Roma, Italy*

[4]*Laboratoire de Chimie Physique–Matière et Rayonnement (UMR 7614), Université Pierre et Marie Curie, 11 rue Pierre et Marie Curie, 75231 Paris Cedex 05, France*

[5]*CNR, Institute for Superconducting and Innovative Materials and Devices (CNR-SPIN), 67100 L'Aquila, Italy*

[6]*Dipartimento di Fisica, Università degli Studi dell'Aquila, Via Vetoio 10, 67010 Coppito (L'Aquila), Italy*

[7]*Institute of Precision Optical Engineering, Department of Physics, Tongji University, Shangai 200092, People's Republic of China*

[8]*UR1-CNRS/Synchrotron SOLEIL, Saint-Aubin, B.P. 48, 91192 Gif-sur-Yvette Cedex, France*

[9]*Synchrotron SOLEIL, Saint-Aubin, B.P. 48, 91192 Gif-sur-Yvette Cedex, France*

[10]*Central Laser Facility, Rutherford Appleton Laboratory, Didcot, Oxon OX11 0QX, United Kingdom*

[11]*Lund University, MAX-lab, P.O. Box 118, 221 00 Lund, Sweden*

(Received 20 December 2012; revised manuscript received 8 March 2013; published 29 April 2013)

Mn_5Ge_3(001) thin films grown on Ge(111)-$c(2 \times 8)$ reconstructed surfaces were studied by angle-resolved photoemission using synchrotron radiation in the 14–94 eV photon energy range. The results obtained in the ΓALM plane and in the ΓAHK plane are in agreement with simulations starting with band structure calculations based on the density functional theory. This provides a unique validation of band structure calculations for a proper description of the electronic properties of Mn_5Ge_3. Only the spectral feature very close to the Fermi level cannot be well explained by the simulation. This departure is discussed in terms of the three-dimensional nature of the sample and of correlation effects.

DOI: 10.1103/PhysRevB.87.165137 PACS number(s): 79.60.−i, 71.20.−b, 73.20.At, 71.18.+y

I. INTRODUCTION

Conventional electronics relies on the control of the electron charge in semiconducting materials. The emerging field of spintronics aims at the use of the spin degree of freedom of the electron in addition to its charge.[1,2] While semiconducting materials, where the transport of the charge of the electron can be controlled, are at the heart of electronics, ferromagnetic materials, where there is an imbalance in the number of spin-up and spin-down occupied electron states, are at the heart of magnetism. The combination of these two aspects in a single material, a magnetic semiconductor, should permit an electric control of spin transport.[3] Compared to conventional semiconductor devices, nonvolatility, increased data processing speed, decreased power consumption, and increased integration are expected advantages of spintronics.

Such magnetic semiconductors should ideally have a Curie temperature (T_C) above ambient temperature and a highly spin-polarized current. In addition, for practical aspects, they should be compatible with the mainstream Si-based technology. For these reasons a lot of attention has been paid in recent years to the Mn-Ge system.

Promising results have been obtained on Mn_xGe_{1-x} diluted magnetic semiconductors,[4] with an expected increase of the T_C with x. But it was soon realized that fabricating Mn_xGe_{1-x} with x greater than a few percent was difficult because of the very limited solubility of Mn in the Ge matrix and the subsequent formation of precipitates of intermetallic compounds, such as Mn_5Ge_3.[5] Recently this ferromagnetic compound has attracted a strong interest because it has a high T_C (≈290 K)[6] and it can be grown epitaxially on Ge(111) substrates,[7] permitting, in principle, a direct injection of the spin-polarized current from the Mn_5Ge_3 film directly into the Ge semiconductor. To shed light on such a possibility, it is important to have a detailed knowledge of the electronic structure of this material.

On the theoretical side, investigations of the bulk electronic and magnetic properties have been performed using the density functional theory.[8–10] In particular, a full-potential linearized augmented plane-wave calculation[8] shows the strong metallic character of Mn_5Ge_3 with a dominant Mn 3*d* contribution from the Fermi level (E_F) down to a binding energy (BE) of 3.5 eV.

On the experimental side, off- and on-resonance (across the Mn 2*p* and 3*p* edges) valence band (VB) photoemission spectroscopy (PES)[11–13] and Mn 2*p* x-ray magnetic circular dichroism measurements[12,13] have been performed. They confirm the metallic character of Mn_5Ge_3 and that the main contribution of the Mn 3*d* states to the electronic density of states is located between E_F and 3 eV BE. Note that spin-resolved PES measurements (He Iα excitation) have revealed a spin polarization at E_F of +15%,[14] in contrast with the −41% value expected from band structure calculations, point-contact Andreev reflection measurements giving a value of +42%.[15] Recently, angle-resolved (AR) PES measurements along the $\overline{\Gamma}$-$\overline{M}$-$\overline{\Gamma}$ and $\overline{\Gamma}$-$\overline{K}$-$\overline{M}$ directions of the surface Brillouin zone (BZ) using He Iα photons have been reported.[16]

In this paper, we present PES measurements at normal electron emission, i.e., along the ΓA direction, and in the ΓALM and ΓAHK planes, on Mn_5Ge_3(001) films epitaxially grown on Ge(111). Although some of us already studied theoretically the electronic structure of Mn_5Ge_3,[8–10] here we consistently recalculate the band structure in order to make easier a direct comparison to the new experimental data.

II. EXPERIMENTAL AND COMPUTATIONAL DETAILS

The intermetallic compound Mn_5Ge_3 has a hexagonal $D8_8$-type crystal structure. The unit cell ($a = 0.718$ and $c = 0.505$ nm) contains 10 Mn and 6 Ge atoms. It contains two crystallographically independent sets of manganese atoms: Mn1 atoms, in a fourfold position with 32 symmetry [4(d) sites], and Mn2, in a sixfold position with *mm* symmetry [6(g) sites]. There is a consensus that the surface is Mn1 terminated.[16] The corresponding structural model, as well as the BZ, are presented in Figs. 1(a) and 1(b), respectively.

The $Mn_5Ge_3(001)$ thin films were grown at room temperature by depositing Mn on Ge(111)-$c(2 \times 8)$ using a calibrated Knudsen cell with a deposition rate of 0.1 nm/min. The Ge(111)-$c(2 \times 8)$ surface was prepared by cycles of sputtering (1 keV Ar^+ ions) of a Ge(111) substrate and annealing at 700 °C, until a sharp low-energy electron diffraction (LEED) pattern was obtained. After Mn deposition (40–50 ML), the sample was annealed for several minutes at 720 K. A sharp $(\sqrt{3} \times \sqrt{3})R30^\circ$ LEED pattern characteristic of an ordered $Mn_5Ge_3(111)$ surface was then obtained [see Fig. 1(c)].

The PES studies were performed at the Cassiopée beamline of the SOLEIL synchrotron radiation facility (Saint-Aubin, France) and at the I3 beamline of MAX-lab (Lund, Sweden). All the experiments were performed at room temperature. The spectra were collected with an acceptance angle of $\approx \pm 14^\circ$ using a Scienta R4000 analyzer. The combined beamline and spectrometer energy resolution was better that 50 meV and the photon energy spans from 14 to 94 eV.

Density functional calculations were performed using the Vienna Ab initio Simulation Package within the generalized gradient approximation.[17] Projector augmented wave pseudopotentials[18,19] were used for both Ge and Mn atoms: the semicore $3p$ states are considered as valence (core) states for Mn (Ge); the $3d$ states are frozen in the core for Ge. The kinetic energy cutoff used for the wave functions was fixed to 350 eV. A $4 \times 4 \times 6$ Γ-centered k-points mesh was used for the self-consistent cycle. All the atomic internal positions were relaxed to minimize the *ab initio* stress and forces.

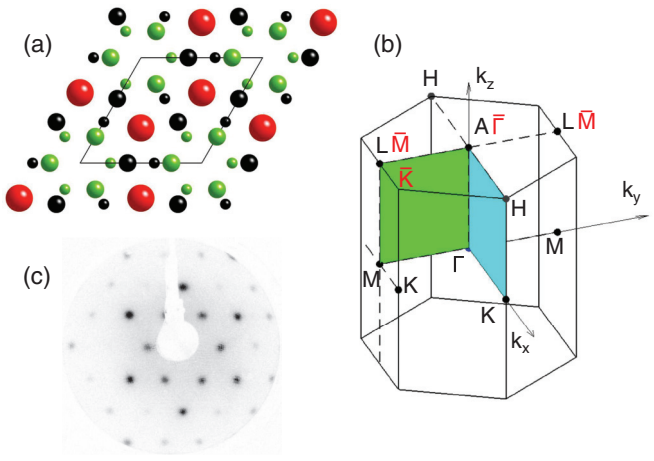

FIG. 1. (Color online) (a) Projection on the (001) plane of the crystal structure of bulk Mn_5Ge_3. Red, green, and black balls are Mn1, Mn2, and Ge atoms, respectively. The unit cell is shown by the line. The large-sized balls correspond to Mn1 atoms at $z = 0$ (and masked Mn1 atoms at $z = 1/2$); the medium- and small-sized balls correspond respectively to $z = 3/4$ and $z = 1/4$ Mn-Ge mixed planes. (b) $(\sqrt{3} \times \sqrt{3})R30^\circ$ LEED pattern of a $Mn_5Ge_3(001)$ film grown on Ge(111)c-(2×8). (c) Mn_5Ge_3 bulk and surface [(red) overlined symbols] BZ showing the main symmetry points and directions. The measurements were done in the ΓALM plane (in light green) and in the ΓAHK plane (in light blue).

III. RESULTS AND DISCUSSION

We measured VB PES spectra at normal emission using photons in the 14–94 eV energy range which allowed us to follow the ΓA symmetry line in the reciprocal space. This energy range covers more than two BZs along this symmetry line. In Fig. 2(a) the spectra measured with photon energies from 58 to 94 eV are shown. Several qualitative observations can be made from a first visual inspection. Three dominant structures, labeled 1, 2, and 3, located close to E_F, at ≈1 eV BE, and at ≈2.3 eV BE, respectively, are observed. All three structures exhibit weak dispersion and intensity variations. In Fig. 2(b) we plot the intensity of the second derivative of the same set of spectra. Clear dispersion is observed for structure 2, whereas structure 3 exhibits only a subtle variation in energy. A closer look reveals also a periodicity in the intensity variation of structure 1 as a function of photon energy [see Fig. 2(c)] that is accompanied by a change in its shape [see Fig. 2(a)]. Structure 1 appears as a clear peak ≈70 and ≈90 eV photon energy, indicating that bands are crossing E_F at the corresponding k points.

From our calculation and in agreement with Ref. 8, the main contribution of the Mn $3d$ states is expected between E_F and 3.5 eV BE, the Ge s-p states being located at higher BE. This is seen in the spectra where, due to large photoionization cross section for d electrons, high photoelectron intensity is observed from E_F up to BEs of ≈3 eV. In this BE range, the calculated dispersions $E(\mathbf{k})$ show a complex entanglement of almost nondispersing Mn $3d$ electron bands that can hardly

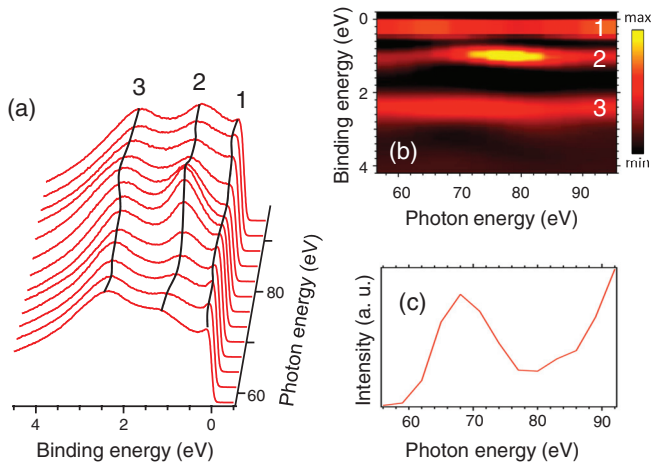

FIG. 2. (Color online) (a) Valence band PES spectra of Mn_5Ge_3 at normal emission. Each spectrum has been normalized to its integral value. Three main structures in the spectra are marked by 1, 2, and 3. The lines, which follow the dispersion of these three structures, are a guide to the eye. (b) Second derivative of the spectra shown in (a). (c) Spectral intensity of structure 1 as a function of the photon energy.

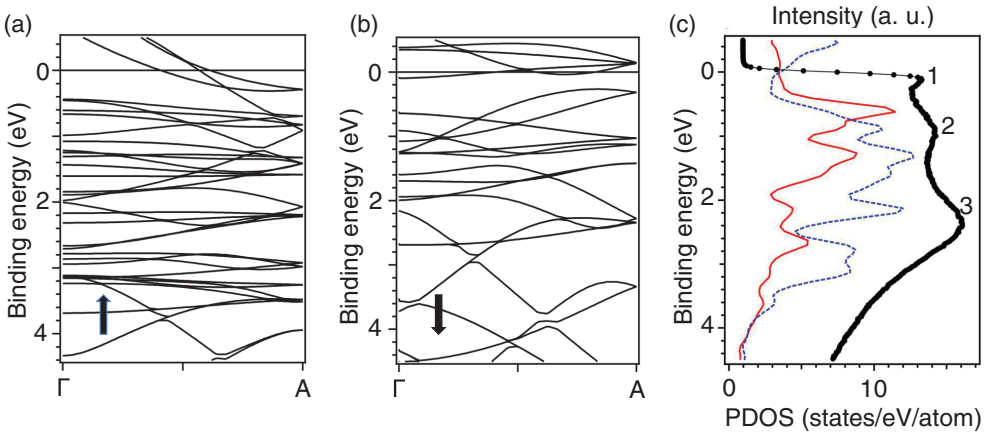

FIG. 3. (Color online) (a) Majority- and (b) minority-spin electron band structure along the ΓA direction, according to our calculation. (c) Mn1 (continuous red line) and Mn2 (dashed blue line) projected densities of states compared to a typical normal emission PES spectrum (measured here with a photon energy of 64 eV) with the three structures 1, 2, and 3.

be resolved individually in PES. In Figs. 3(a) and 3(b) we show calculated band structure along the ΓA symmetry line for majority- and minority-spin electrons, respectively. A more pronounced dispersion of bands is observed only in a narrow energy region between E_F and ≈0.7 eV BE. Here are located electronic states resulting from hybridization between Mn1 and Mn2 3*d* electrons and between Mn 3*d* and Ge 4*p* electrons. Three majority electron bands are crossing E_F, so one would expect clear peaks in PES spectra in the middle of the ΓA line [see Fig. 3(a)]. This is observed to some extent, as shown in Fig. 2(a), but, surprisingly, the peaks are superimposed on a nonvanishing intensity at E_F that is spread out through the whole BZ. The intensity is seemingly due to flat minority electron bands, almost parallel to the Fermi level [Fig. 3(b)], in such a way that they are expected to contribute here in a constant manner. Similarly, the persistence of a Fermi edge has been observed in PES spectra recorded in angular mode with a single photon energy of 21 eV (He Iα excitation).[16] High photoemission intensity at E_F was measured in various Mn-based compounds as well, such as MnSb.[20]

This nonvanishing intensity at E_F can additionally be generated by other processes. One of them is an intrinsic property of three-dimensional (3D) systems, as is the case for Mn_5Ge_3. Due to inelastic scattering, the extension of the photoemission final-state wave function into the crystal interior is limited to the electron mean free path, which is of the order of a few angstroms. Such a confinement in the surface-perpendicular coordinate results in an intrinsic uncertainty in the surface-perpendicular momentum ($k_\perp$), described by its broadening of the order of a few tenths of the BZ extension. This gives rise to a significant distortion in the PE signal from the bands with $k_\perp$ dispersion.[21,22] As a consequence, PE intensity appears at E_F even in the absence of bands at E_F. A presence of surface states can bring some intensity, too. This will be discussed later on.

There are also other effects requiring an approach beyond the one-electron picture. A coupling of charge and bosonic degrees of freedom, such as phonons, polarons, and magnons, are all known to be important in solids.[23] Mn_5Ge_3 being a magnetic material, coupling to magnon modes has been identified recently by infrared spectroscopy.[24] Their interaction energy is estimated to be ≈60 meV. In Mn-based diluted magnetic semiconductors the development of the ferromagnetic state has been attributed to percolation of magnetically ordered regions, described as bound magnetic polarons.[25] These are likely to exist also in Mn_5Ge_3.

As already pointed out, the most pronounced dispersion is observed for peak 2. At the corresponding BEs, the only electronic states having a high density and a non-negligible photoionization cross section are the Mn 3*d* states. As the high density of states is due to flat *d* bands, in a first step, a comparison between experiment and calculation can be made on the basis of Mn projected densities of states (PDOS). This is shown in Fig. 3(c) where the Mn1 and Mn2 3*d* PDOS are compared to a typical PES spectrum (the displayed PES spectrum has been measured with a photon energy of 64 eV). This allows us to understand the correspondence between the 1, 2, and 3 structures and the respective PDOS where peak 2 results mainly from Mn1 3*d* and Mn2 3*d* interaction; peak 3 is due mostly to Mn2 3*d* electrons. At this point, it is important to recall that in the complex structure of Mn_5Ge_3, Mn1 atoms have 6 Ge neighbors (at 2.53 Å), whereas Mn2 atoms have 5 Ge neighbors (2, 1, and 1 at 2.48, 2.61, and 2.76 Å, respectively). Thus hybridization between Mn and Ge atoms is expected to be stronger for Mn1 atoms than for Mn2 atoms; as a consequence, Mn1 3*d* electrons will have a more pronounced dispersion. This is corroborated by the experimental observation that peak 3 disperses much less than peak 2.

Observed dispersions in normal emission allow in principle to set the correspondence between the photon energy and a position in the bulk BZ. This task appears, however, to be rather delicate in Mn_5Ge_3. Several majority- and minority-spin bands cross E_F along the ΓA symmetry line [see Figs. 3(a) and 3(b)]. Referring to the calculated bands one can qualitatively expect lower spectral intensity in the vicinity of both Γ and A points at E_F. In fact, we observe oscillations of the spectral intensity at E_F, as shown in Fig. 2(a), and, at intensity maxima, the peak at E_F becomes sharper (photon energies of 65–70 and 90–94 eV), indicating the presence of bands crossing E_F. Based on this observation and using the free-electron model

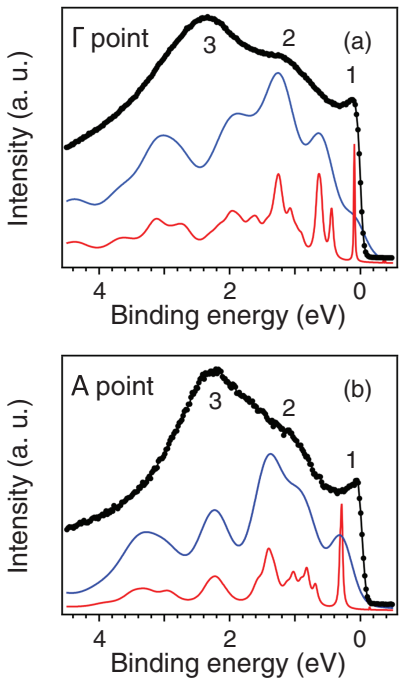

FIG. 4. (Color online) Comparison between theory and experiment for PES spectra measured in the vicinity of the Γ [panel (a)] and A points [panel (b)], i.e., with photon energies of 41 and 60 eV, respectively. The red curves show the simulation taking into account the Lorentzian lifetime broadening only; the blue curves include also a convolution by a Gaussian with a FWHM of 400 meV. See text for details.

for final states, we deduce a value of 12.4 eV for the inner potential V_0, defined by $k_z \propto \sqrt{\hbar\omega + V_0}$. Consequently, the Γ and A points correspond to photon energies of 41 and 82 eV, and of 24 and 60 eV, respectively.

For an unambiguous correspondence between photon energies and Γ and A points, a key step is a comparison of measured spectra with calculations. Because at present the calculation of the photoemission process is difficult for complex systems such as Mn_5Ge_3, we did a simulation of the spectra using a simple model. We used the free-electron approximation for the final states, ignoring the matrix elements. In the simulation, the ground state theoretical data were convoluted by Lorentzian and Gaussian functions to account for photohole lifetime effects and for $k_\perp$ broadening plus correlation effects, respectively. A reasonable description of the initial-state lifetime broadening was found using a Lorentzian with a full width at half maximum ($FWHM_L$) varying linearly from 0 at E_F to 1 eV at 8 eV BE. A $FWHM_G$ of 400 meV was found to give the best agreement with the experiment. In Fig. 4 we show such a comparison for the Γ [Fig. 4(a)] and A [Fig. 4(b)] points with measured spectra at photon energies of 41 and 60 eV, respectively. Red curves stand for band calculation convoluted by the Lorentzian profile only; blue curves include also the convolution by the Gaussian profile. The agreement between the positions of observed structures 1, 2, and 3 and those given by the simulation is satisfactory. However, as the differences between the Γ and A point PES spectra (and simulations) are faint, the attribution of the respective symmetry points can still be questionable.

The final cross-check is achieved from the overall behavior of dispersions along high-symmetry lines. This is shown in Fig. 5 where we compare the second-derivative ARPES intensity (left panels) with the calculated bands (right panels) in the ΓM [Figs. 5(a) and 5(b)] and AL [Figs. 5(c) and 5(d)] directions. A second-derivative representation is used to amplify the structures 1, 2, and 3. Here, the calculated bands are

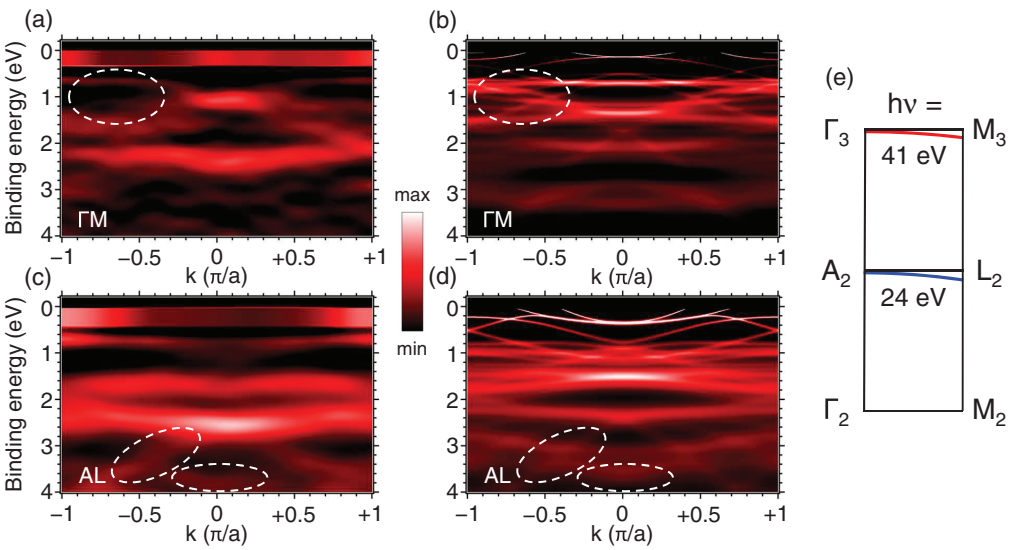

FIG. 5. (Color online) Band dispersion along the ΓM [(a) and (b)] and AL [(c) and (d)] lines. Left panels: second derivative intensity plot of the ARPES spectra. Right panels: calculated bands convoluted by the Lorentzian function representing the contribution of the photohole lifetime. The dotted lines point out the spectral regions that are characteristic of a given high symmetry line but, at the same time, different between the respective lines. Panel (e) shows the trajectories followed in the k space in off-normal photoemission for the photon energies of 41 and 24 eV (see text for details).

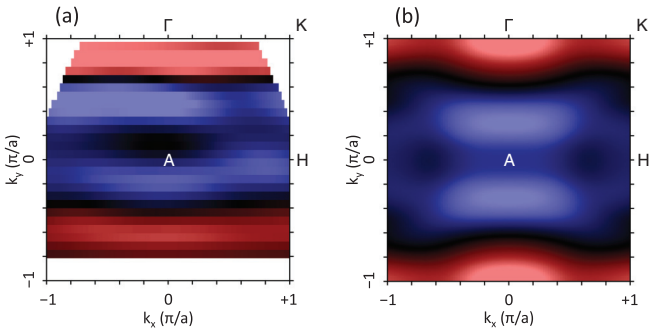

FIG. 6. (Color online) Constant binding energy surface at BE = 2.2 eV (peak 3) in the ΓAHK plane: (a) experiment; (b) simulation.

convoluted only by the Lorentzian function for the photohole lifetime contribution. ARPES data were measured with a photon energy of 41 and 24 eV for the ΓM and AL directions, respectively. At this point it needs to be stressed that using a constant photon energy one cannot follow exactly the ΓM (AL) direction in off-normal photoemission. In our experimental conditions the deviation is, however, very small, about 5% for $\hbar\omega = 24$ eV [see Fig. 5(e)]. Due to the weak dispersions caused by flat bands, this deviation can be neglected.

Structure 1 contains bands in the 0–0.5 eV BE range with relatively steeper dispersion than in structures 2 and 3. Even the second-derivative procedure does not allow us to obtain details about any of the individual bands. The strongest dispersion with a nice periodicity is exhibited by structure 2. This structure is clearly reproduced in the calculations in the BE region between ≈0.5 and ≈1.5 eV BE. At higher BE, the most significant spectral intensity contribution is brought by structure 3, built up essentially by Mn2 3*d* electrons, as already discussed. The dotted lines in Figs. 5(a)–5(d) show the regions exhibiting clear differences between the spectra and at the same time well corresponding to simulations allowing an unambiguous distinction between the high-symmetry lines. We find as well good resemblance of the principal features between ARPES spectra and simulations for the ΓK line and the AH line (not shown here).

As seen in the above discussion an overall agreement between theory and experiment is achieved. Thus, the ARPES spectra can be interpreted by bulk band electronic structure. The presence of any surface states cannot be confirmed from our data.

ARPES studies are extremely useful to determine the Fermi surface, which contains key information about thermal, electrical, magnetic, and optical properties. More fundamentally, experimental Fermi-surface measurements are a crucial test for calculations. In our case, as already mentioned, the structure 1 near E_F does not correspond to the calculated bands for most spectra. We have discussed and brought forward above as one possible reason correlation effects and electron-polaron interaction. In addition electronic surface states may as well be present. With these considerations in mind, it is not surprising that our experimental Fermi surface (not shown) does not fit to the simulation (made using the same simple model as used previously to simulate the ARPES spectra) from the calculated band structure. Thus we have preferred to plot the surface of constant BE corresponding to structure 3 in the ΓAHK plane. In Figs. 6(a) and 6(b), we compare our experimental surface for peak 3 with the calculated one. For the presentation, the photoemission intensity is integrated over an energy window of 150 meV around the BE of 2.2 eV [Fig. 6(a)]. The same procedure is applied to the simulated intensity, shown in Fig. 6(b). Comparing the two images, we find a very good overall agreement of the distribution of maxima and minima. This represents quite a critical test since it concerns a whole plane in the 3D BZ, while the other spectra presented above concerned either individual points or high-symmetry lines in reciprocal space. For peak 2 we obtain as well good agreement between measured and simulated constant energy surfaces.

IV. CONCLUSIONS

We have investigated the electronic structure of Mn_5Ge_3 thin films by ARPES. The spectra were compared to density functional band structure calculations after application of a simple simulation of the photoemission process. A good agreement between theory and experiment is found, demonstrating that band structure calculations are suitable to describe the electronic properties of Mn_5Ge_3. This allowed us also to evidence low contribution of surface states to measured spectra. Finally, our results suggest the importance of electron-boson (probably polaron) as well as the influence of $k_\perp$ broadening, in the explanation of the spectral weight at the Fermi level.

ACKNOWLEDGMENTS

The research leading to these results has received funding from the European Community's Seventh Framework Programme (FP7/2007-2013) under Grant Agreement No. 226716. We acknowledge the CINECA award under the ISCRA initiative, for the availability of high-performance computing resources and support. Computational resources from the CASPUR supercomputing center (Rome) are also acknowledged.

[1] F. Pulizzi, Nat. Mater. **11**, 367 (2012).
[2] S. D. Bader and S. S. P. Parkin, Annu. Rev. Condens. Matter Phys. **1**, 71 (2010).
[3] S. Datta and B. Das, Appl. Phys. Lett. **56**, 665 (1990).
[4] Y. D. Park, A. T. Hanbicki, S. C. Erwin, C. S. Hellberg, J. M. Sullivan, J. E. Mattson, T. F. Ambrose, A. Wilson, G. Spanos, and B. T. Jonker, Science **295**, 651 (2002).
[5] C. Bihler, C. Jaeger, T. Vallaitis, M. Gjukic, M. S. Brandt, E. Pippel, J. Woltersdorf, and U. Gösele, Appl. Phys. Lett. **88**, 112506 (2006).
[6] R. Fontaine and R. Pauthenet, C. R. Acad. Sci. **254**, 650 (1962).
[7] See for instance: P. De Padova, J.-M. Mariot, L. Favre, I. Berbezier, B. Olivieri, P. Perfetti, C. Quaresima, C. Ottaviani, A. Taleb-Ibrahimi, P. Le Fèvre, F. Bertran, O. Heckmann, M. C. Richter,

W. Ndiaye, F. D'Orazio, F. Lucari, C. M. Cacho, and K. Hricovini, Surf. Sci. **605**, 638 (2011), and the references cited therein.
[8]S. Picozzi, A. Continenza, and A. J. Freeman, Phys. Rev. B **70**, 235205 (2004).
[9]A. Stroppa and M. Peressi, Mater. Sci. Semicond. Proc. **9**, 841 (2006).
[10]A. Stroppa and M. Peressi, Phys. Status Solidi A **204**, 44 (2007).
[11]C. Zeng, W. Zhu, S. C. Erwin, Z. Zhang, and H. H. Weitering, Phys. Rev. B **70**, 205340 (2004).
[12]P. De Padova, J.-P. Ayoub, I. Berbezier, P. Perfetti, C. Quaresima, A. M. Testa, D. Fiorani, B. Olivieri, J.-M. Mariot, A. Taleb-Ibrahimi, M. C. Richter, O. Heckmann, and K. Hricovini, Phys. Rev. B **77**, 045203 (2008).
[13]L. Sangaletti, G. Drera, E. Magnano, F. Bondino, C. Cepek, A. Sepe, and A. Goldoni, Phys. Rev. B **81**, 085204 (2010).
[14]Yu. S. Dedkov, M. Holder, G. Mayer, M. Fonin, and A. B. Preobrajenski, J. Appl. Phys. **105**, 073909 (2009).
[15]R. P. Panguluri, C. Zeng, H. H. Weitering, J. M. Sullivan, S. C. Erwin, and B. Nadgorny, Phys. Status Solidi B **242**, R67 (2005).
[16]J. H. Grytzelius, H. M. Zhang, and L. S. O. Johansson, Phys. Rev. B **84**, 195306 (2011).
[17]J. P. Perdew, K. Burke, and M. Ernzerhof, Phys. Rev. Lett. **77**, 3865 (1996).
[18]P. E. Blöchl, Phys. Rev. B **50**, 17953 (1994).
[19]G. Kresse and D. Joubert, Phys. Rev. B **59**, 1758 (1999).
[20]O. Rader, A. Kimura, N. Kamakura, K.-S. An, A. Kakizaki, S. Miyanishi, H. Akinaga, M. Shirai, K. Shimada, and A. Fujimori, Phys. Rev. B **57**, R689 (1998).
[21]V. N. Strocov, J. Electron Spectrosc. Relat. Phenom. **130**, 65 (2003).
[22]J. Krempaský, V. N. Strocov, L. Patthey, P. R. Willmott, R. Herger, M. Falub, P. Blaha, M. Hoesch, V. Petrov, M. C. Richter, O. Heckmann, and K. Hricovini, Phys. Rev. B **77**, 165120 (2008).
[23]*Polarons in Advanced Materials*, edited by A. S. Alexandrov, Springer Series in Material Science, Vol. 103 (Springer, Berlin, 2007).
[24]S. V. Dordevic, L. W. Kohlman, N. Stojilovic, Rongwei Hu, and C. Petrovic, Phys. Rev. B **80**, 115114 (2009).
[25]A. Kaminski and S. Das Sarma, Phys. Rev. Lett. **88**, 247202 (2002).